Synaptic muscarinic response types in hippocampal CA1 interneurons depend on different levels of presynaptic activity and different muscarinic receptor subtypes

L. Andrew Bell, **Karen A. Bell**, and **A. Rory McQuiston**[*]

Department of Anatomy and Neurobiology, Virginia Commonwealth University, School of Medicine, Richmond, VA 23298, USA

Abstract

Depolarizing, hyperpolarizing and biphasic muscarinic responses have been described in hippocampal inhibitory interneurons, but the receptor subtypes and activity patterns required to synaptically activate muscarinic responses in interneurons have not been completely characterized. Using optogenetics combined with whole cell patch clamp recordings in acute slices, we measured muscarinic responses produced by endogenously released acetylcholine (ACh) from cholinergic medial septum/diagonal bands of Broca inputs in hippocampal CA1. We found that depolarizing responses required more cholinergic terminal stimulation than hyperpolarizing ones. Furthermore, elevating extracellular ACh with the acetylcholinesterase inhibitor physostigmine had a larger effect on depolarizing versus hyperpolarizing responses. Another subpopulation of interneurons responded biphasically, and periodic release of ACh entrained some of these interneurons to rhythmically burst. M4 receptors mediated hyperpolarizing responses by activating inwardly rectifying K^+ channels, whereas the depolarizing responses were inhibited by the nonselective muscarinic antagonist atropine but were unaffected by M1, M4 or M5 receptor modulators. In addition, activation of M4 receptors significantly altered biphasic interneuron firing patterns. Anatomically, interneuron soma location appeared predictive of muscarinic response types but response types did not correlate with interneuron morphological subclasses. Together these observations suggest that the hippocampal CA1 interneuron network will be differentially affected by cholinergic input activity levels. Low levels of cholinergic activity will preferentially suppress some interneurons via hyperpolarization and increased activity will recruit other interneurons to depolarize, possibly because of elevated extracellular ACh concentrations. These data provide important information for understanding how cholinergic therapies will affect hippocampal network function in the treatment of some neurodegenerative diseases.

Keywords

Hippocampus; Medial septum/diagonal band of Broca; complex; Muscarinic synaptic potentials; Optogenetics; Interneuron

1. Introduction

Information processing by hippocampal CA1 includes coding of spatial information and episodic memory formation (Moscovitch et al., 2006), both processes that are important for behavioral functioning. These tasks rely on hippocampal inhibitory interneurons that control

[*]Corresponding author. Department of Anatomy and Neurobiology, Virginia Commonwealth University, Box 980709, Richmond, VA 23298, USA. Tel.: +1 804 828 1573; fax: +1 804 828 9477. amcquiston@vcu.edu (A.R. McQuiston).

synaptic input, dendritic integration and output of CA1 pyramidal neurons (Maurer et al., 2006; Hangya et al., 2010; Royer et al., 2012). The functioning of this network in part depends on acetylcholine (ACh) inputs from the medial septum and diagonal bands of Broca (MS/DBB). Disruption of the MS/DBB input by systemic blockade of muscarinic cholinergic receptors or direct injection of muscarinic receptor antagonists into the hippocampus can impair memory (Atri et al., 2004; Hasselmo, 2006) and the encoding of spatial information (Blokland et al., 1992).

Most studies examining the role of ACh input onto hippocampal interneurons *in vitro* have involved exogenous application of cholinergic agonists (Bonner, 1989; McQuiston and Madison, 1999a; Lawrence et al., 2006; Cea-del Rio et al., 2010; Chiang et al., 2010; Cea-del Rio et al., 2011; Zheng et al., 2011) or electrical stimulation of cholinergic fibers (Widmer et al., 2006; Gu and Yakel, 2011). However, exogenous cholinergic agonist application cannot mimic the temporal or spatially variable concentrations of ACh that arise from synaptic release (Parikh et al., 2007; Zhang et al., 2010). Furthermore, electrical stimulation may only activate a subset of axons surrounding the stimulating electrode, potentially preventing the generation of cholinergic responses in some interneuron subtypes. Therefore, conclusions regarding interneuron function in studies using these methods may give an incomplete or an inaccurate picture. In contrast, using optogenetics to control ACh synaptic release in brain slices directly assesses interneuron function on the hippocampal network (Bell et al., 2011; Gu and Yakel, 2011; Nagode et al., 2011).

Previous studies have shown that CA1 interneurons have different types of muscarinic responses, depolarizing, hyperpolarizing, or biphasic responses (hyperpolarization followed by depolarization) (McQuiston and Madison, 1999a; Widmer et al., 2006). However, the precise location of CA1 interneuron subtypes that differentially respond to synaptically released ACh is incompletely understood. Furthermore, it is unclear what types of pre-synaptic activity patterns are required to produce the different response types, and it is not known what subtypes of muscarinic receptors mediate these responses. Combining optogenetic tools and whole cell patch clamping, we recorded from interneurons in hippocampal CA1 with fast hyperpolarizations, slow depolarizations, and biphasic responses resulting from endogenous ACh release. Interestingly, hyperpolarizing responses required less cholinergic presynaptic activity compared to depolarizing responses. Pharmacologically, M_4 receptors were involved in mediating the hyperpolarization. In addition, we found a subset of interneurons displaying biphasic responses that could be selectively entrained by rhythmic activation of cholinergic inputs. Our findings demonstrate that hippocampal activity may be differentially modulated by recruiting or suppressing different subtypes of inhibitory interneurons through varying patterns of cholinergic activity from MS/DBB input.

2. Methods

2.1. Animals

The 134 B6; 129S6-*Chat*[tm1(cre)Lowl]/J (Chat-cre, JAX Stock No. 006410) mice used in these studies were housed in an animal care facility approved by the American Association for the Accreditation of Laboratory Animal Care (AAALAC). Animal experimental procedures followed a protocol approved by the Institutional Animal Care and Use Committee of Virginia Commonwealth University (AD 20205). This protocol adhered to the ethical guidelines described in The Care and Use of Laboratory Animals 8th Edition (Garber, 2011). All efforts were made to minimize animal suffering and to reduce the number of animals used.

2.2. Generation and stereotaxic injection of rAAV-Flex-rev-oChIEF-tdTomato into the MS/DBB of Chat-cre mice

A recombinant adeno-associated virus (rAAV, serotype 1 or 9) expressing FLEXed oChIEF-tdTomato was generated using a previously described method (Bell et al., 2011) in order to selectively express oChIEF-tdTomato in infected cells that also expressed Cre recombinase. Mice were initially anesthetized via intraperitoneal injection of ketamine (100 mg/kg IP) and xylazine (2.5 mg/kg IP). Anesthesia was maintained with O_2 supplemented with 1.0% isoflurane. An incision was made in the skin along the midsagittal suture, and a small hole was drilled in the skull overlying the septum. An aluminosilicate glass pipette containing rAAV-Flex-rev-oChIEF-tdTomato was lowered to the level of the MS/DBB, approximately 0.8–1.0 mm rostral to Bregma and infused at a rate of 100 nl/min using a software driven injectomate (Neurostar, Sindelfingen, Germany). In total, 8×100 nl injections were made between 3.5 and 5.0 mm in depth. 10–15 days post viral injection, 38–56 day old mice were sacrificed for experimentation.

2.3. Preparation of hippocampal slices

Brain slices were obtained by methods previously described (Bell et al., 2011). In brief, horizontal slices containing the mid-temporal hippocampus were cut at 350 μm on a Leica VT1200 (Leica Microsystems, Buffalo Grove, IL). Sections were incubated in a holding chamber kept at 36 °C for 30 min and then allowed to return to room temperature. The holding and recording chamber solution consisted of normal saline (in mM): NaCl 125, KCl 3.0, $CaCl_2$ 1.2, $MgSO_4$ 1.2, $NaHPO_4$ 1.2, $NaHCO_3$ 25, glucose 25 bubbled with 95% O_2/5% CO_2. Recordings were performed at 32–34 °C.

2.4. Light-evoked release of acetylcholine from MS/DBB cholinergic axon terminals

Cholinergic terminals expressing oChIEF-tdTomato were stimulated by blue light transmitted through the epi-illumination light path of an Olympus BX51WI microscope and a 20× water immersion objective (0.95 NA). Blue light flashes (1 ms in duration) were generated either from a flash lamp (JML-C2, Rapp Optoelectronic) by passing light through a D455/70 excitation filter focused into a liquid light guide or from a light-emitting diode (LED) (UHP-microscope-LED-460, Prizmatix Modiin-Ilite, Givat Shmuel, Israel). Blue light exiting the light guide or LED was focused into the epi-illumination light path of the Olympus BX51WI microscope and back aperture of the 20× water immersion objective (0.95 NA) using an optiblock beam combiner (Prizmatix) or a Flashcube 70 (Rapp Optoelectronics, Hamburg, Germany) and two dichroic mirrors (515dcxru, Chroma Technology, Bellows Falls, VT, USA).

2.5. Electrophysiological measurements

Whole cell patch clamp recordings on hippocampal CA1 interneurons were performed using patch pipettes (2–5 MΩ) pulled from borosilicate glass (8250 1.65/1.0 mm) on a Narishige PC-10 pipette puller filled with (in mM): $KMeSO_4$ 135, NaCl 8, MgATP 2, NaGTP 0.1, HEPES 10, $BAPTAK_4$ 0.1, biocytin 0.1%. Membrane potentials were measured with a Model 2400 patch clamp amplifier (A-M Systems, Port Angeles, WA) and converted into a digital signal by a PCI-6040E A/D board (National instruments, Austin, TX). WCP Strathclyde Software was used to store and analyze membrane potential responses on a PC computer (courtesy of Dr. J Dempster, Strathclyde University, Glasgow, Scotland). Further analysis was performed with Originpro 8.1 (OriginLab Corp., Northampton, MA, USA), Excel (Microsoft, Redmond, WA) and SPSS 20.0 (IBM, Armonk, NY). To evoke synaptic electrical activity in hippocampal CA1, bipolar platinum-iridium stimulating electrodes (approx. 100 kΩ, FHC Inc., Bowdoin, ME, USA) were placed in Shaffer collaterals of CA3 pyramidal neurons.

2.6. Morphological reconstruction of interneurons displaying muscarinic synaptic responses

Slices were fixed, washed and incubated with streptavidin Alexa Fluor 633 (Life Technologies, Invitrogen) as previously described (Bell et al., 2011). Processed slices were then reconstructed using a Zeiss LSM 710 confocal microscope (Carl Zeiss, Jena, Germany). Alexa 633 was excited with the 633 nm line of a HeNe 5 mW laser and cells were visualized using a 20× dry lens (0.8 N.A., voxel dimensions 0.2 0.2 1.1 μm). The imaged interneurons were traced using the Autoneuron module within the Neurolucida program (MBP, Burlington, VT).

2.7. Statistics and data analysis

Data were analyzed using WCP software for the electrophysiological measurements. Statistics were performed using SPSS 20.0 (IBM, Armonk, NY). Statistical significances for groups of 3 or more were determined using a one-way ANOVA or repeated measures ANOVA with Bonferroni *post hoc* tests or a Fisher's exact test. Statistical significances for groups of 2 were determined with two-tailed *t*-tests. Differences were determined to be statistically significant for *p* values less than 0.05. All data was reported as the mean, standard error of the mean (SEM). Asterisks were as follows unless otherwise noted, ***$p <$ 0.001, **$p <$ 0.01, *$p <$ 0.05.

2.8. Chemicals

All chemicals were purchased from VWR unless otherwise indicated. VU 0255035 (M_1-selective antagonist), VU 0357017 (M_1-selective positive allosteric modulator), VU 10010 (M_4-selective positive allosteric modulator), and VU 0238429 (M_5-selective positive allosteric modulator) were obtained from Tocris Bioscience (Ellisville, Missouri) and 6,7-Dinitroquinoxaline-2,3-dione (DNQX), DL-2-Amino-5-phosphono pentanoic acid (APV) from Ascent Scientific (Bristol, U.K.). Biocytin (B-1592) was purchased from Life Technologies (Invitrogen).

3. Results

Using optogenetics, we investigated cholinergic synaptic transmission onto hippocampal CA1 interneurons in acute brain slices by selectively expressing the excitatory optogenetic protein oChIEF-tdTomato (Lin et al., 2009) in MS/DBB cholinergic terminals. A recombinant adeno-associated virus (rAAV) containing a FLEXed (Schnütgen et al., 2003) coding sequence for oChIEF-tdTomato was injected into the MS/DBB of mice that expressed Cre recombinase under the control of the choline acetyltransferase promoter (Chat) (Bell et al., 2011). Because the sequence coding for oChIEF-tdTomato was reversed and floxed by two incompatible LoxP sites (Schnütgen et al., 2003), oChIEF-tdTomato expression was limited to cells that also expressed Cre recombinase (i.e. cholinergic neurons – approximately 37% of Chat-expressing neurons). Ten to 14 days after infection, long range projecting oChIEF-tdTomato-labeled fibers were visible in mid-temporal hippocampal slices and synaptic release of ACh could be elicited by full-field (20×, 0.95 NA objective) blue light flashes (1 ms).

3.1. Muscarinic responses in CA1 interneurons: different response types require different presynaptic activity and have different kinetics

In examining the different types of synaptic muscarinic responses in CA1 interneurons, we first explored the number of stimuli (blue light flashes) required to produce each type of response in addition to measuring their response kinetics. We used two stimulus patterns, one that used a small number of pulses (10 pulse at 20 Hz) (Fig. 1 B–D, blue vertical bars) and the other a larger number of pulses (120 pulses at 20 Hz) (Fig. 1G–I). Using only 10

stimuli, we recorded three types of muscarinic synaptic responses in current clamp, fast hyperpolarization (Fig. 1B), slow depolarization (Fig. 1C), and biphasic responses (consisting of a fast hyperpolarization phase followed by a slow depolarization phase, Fig. 1D). The average maximum amplitude of the hyperpolarizing response (-3.01 ± 0.31 mV) was larger than the depolarizing response (1.89 ± 0.22 mV) (Fig. 1E). Fitting the response rise and decay phases with single exponentials we found that hyper-polarizing responses had faster rise (473.3 ± 28.7 ms) and decay time constants (1829.6 ± 129.2 ms) than depolarizing responses (rise: 686 ± 44.3 ms: decay: 3092.7 ± 493.3 ms) (Fig. 1F). Longer burst durations (120 ± 20 Hz) were required to confirm the presence of a biphasic response because at 10×20 Hz stimulation, 45% of biphasic cells had only a hyperpolarizing component. Importantly, some interneurons that produced depolarizing responses were capable of producing actions potentials (Fig. 1H, inset) only when longer bursts were applied to the slice (120×20 Hz).

3.2. Hyperpolarizing responses to synaptic release of ACh are mediated by M_4 and not M_1 or M_5 receptors

There are five subtypes of muscarinic receptors, M_{1-5} (Bonner, 1989), all of which can found at different levels of expression in the hippocampus (Volpicelli and Levey, 2004; Moscovitch et al., 2006). M_2 and M_4 receptors are coupled to G_i proteins and most likely activate inwardly rectifying potassium channels that generate hyperpolarizing responses (Maurer et al., 2006; Widmer et al., 2006; Brown, 2010; Hangya et al., 2010; Royer et al., 2012). Using a new highly selective M_4 positive allosteric modulator (PAM) VU 10010 ($EC_{50} = 400$ nM, with no effect on other muscarinic receptors) (Shirey et al., 2008), we found that most hyperpolarizing responses (71.4%, 20 of 28) were potentiated ($>10\%$ increase of amplitude) by bath application at 5 μM VU 10010 (Fig. 2A). These data suggest that the majority of the synaptic muscarinic hyperpolarizing responses were mediated at least in part by the activation of M_4 receptors.

In order to demonstrate that network responses from neighboring inhibitory and excitatory cells were not contributing to the hyperpolarizing responses, we blocked glutamatergic and GABAergic synaptic transmission by bath applying NMDA/AMPA antagonists (APV, 50 μM and DNQX, 30 μM, respectively) and $GABA_{A-B}$ antagonists (bicuculine 25 μM, CGP 55845 10 μM, respectively) (Fig. 2B). Neither glutamate nor GABA receptor antagonists had a significant effect on amplitude (Fig. 2D) nor on the rise/decay times of responses to synaptically released ACh (data not shown). In contrast, bath application of the nonselective muscarinic antagonist atropine (5 μM) blocked all hyperpolarizing responses (Fig. 1B, G, 2D, E).

Bath application of M_4 PAM significantly increased the amplitude of both the hyperpolarizing response to short burst (10×20 Hz) ($68.2\% \pm 15\%$ of control) and long burst (120×20 Hz) ($47.9\% \pm 13\%$ of control) stimulated release of ACh (Fig. 2A, E). M_4 PAM had the same relative effect in both stimulation protocols (Fig. 2D). In addition to increasing amplitude, M_4 PAM also significantly prolonged the decay time constant of the hyperpolarizing response ($61\% \pm 17$) (Fig. 2E, F) for both types of stimulation protocols (120×20 Hz not shown).

We next tested whether M_1 receptors contributed to the hyperpolarizing responses using the new highly selective M_1 antagonist VU 0255035, (IC_{50} 132.6 ± 28.5 nM, greater than 75 fold more efficacious than all other muscarinic receptors, $IC_{50} > 10$ μM) (Sheffler et al., 2009). Bath application of 5 μM VU 0255035 did not block the hyperpolarizing response nor did it alter the kinetics of the response (Fig. 2B, D). Furthermore, bath application of the highly selective M_5 PAM VU 0238429 (10 μM) (IC_{50} 1.16 μM with >30-fold selectivity over M_1 and M_3 and no efficacy at M_2 or M_4 receptors) (Bridges et al., 2009) also did not

alter the amplitude or the kinetics of the response (Fig. 2C, D). In order to determine the identity of the current responsible for the hyperpolarization, responses were recorded while the cell was voltage clamped at different membrane potentials, from -50 mV to -120 mV (Fig. 2G). The I–V plot indicated an inwardly rectifying current with a reversal potential of -105.9 mV, near the estimated reversal potential of K^+ (-100.4 mV, Fig. 2H). Therefore, hyperpolarizing synaptic responses activated an inwardly rectifying potassium channel through M_4 receptor activation.

To ensure that the lack of M_1 mediated responses in hippocampal interneurons was not due to an ineffective M_1 antagonist, we tested whether VU 0255035 could block a known M_1 receptor mediated response in the hippocampus. It has previously been shown that bath application of carbachol could induce an ADP (afterdepolarization) mediated by M_1 receptors in CA1 pyramidal neurons (Dasari and Gulledge, 2011). We applied a 250–300 pA depolarizing step to CA1 pyramidal neurons and measured the area of the membrane potential following the current step (Fig. 2I, K). In control conditions, most pyramidal neurons had little to no ADP (Fig. 2J, L black trace) but after 3 min of bath application of 10 μM carbachol an ADP emerged (Fig. 2J, L purple traces) in most CA1 pyramidal neurons (14 of 16). The area of the ADP was measured 3 and 15 min after carbachol bath application and no measureable decrease of the ADP was found between those two time points (Fig. 2M). In subsequent experiments, 5 min after a carbachol-induced ADP emerged, VU 0255035 (5 μM) was bath applied in the presence of carbachol. Within 3 min VU 0255035 completely blocked the carbachol-induced ADP (Fig. 2K, L, M). Therefore, these data demonstrate that VU 0255035 is an effective M_1 antagonist in mouse hippocampal slices.

3.3. Muscarinic depolarizing responses in CA1 interneurons are not dependent on M_1, M_4 or M_5 receptors

Anatomical studies have reported that the M_1 subtype is the most prevalent muscarinic receptor subtype in the hippocampus (Levey et al., 1995) and may be the primary mediator of cholinergic effects on cognition (Fornari et al., 2000; Caccamo et al., 2006; Soares et al., 2006). To investigate whether the M_1 receptor is responsible for depolarizing responses in CA1 interneurons, the new highly selective M_1 antagonist VU 0255035 (5 μM) or positive allosteric modulator VU 0357017 (M_1 PAM, 5 μM, EC_{50} = 830 nM, all other muscarinic receptors EC_{50} > 30 μM) (Bridges et al., 2010) were bath applied to examine their effect on depolarizing responses. The M_1 PAM failed to alter the amplitude or kinetics of the depolarizing response in any interneuron (Fig. 3C, D), and the M_1 antagonist had no effect on the depolarizing response to either long (Fig. 3B, D) or short burst stimuli (Fig. 3E, F) in most cells (n = 21 out of 22). In addition to the ineffectiveness of the M_1 receptor pharmacology, both the M_4 (Fig. 3B) and M_5 (Fig. 3C) PAMs did not significantly alter the amplitude (Fig. 3B–E) or kinetics of the depolarizing response. While M_1, M_4, and M_5 receptor pharmacological manipulation failed to have a significant effect on nearly all depolarizing responses, the amplitude of the depolarizing response to both short burst (Fig. 3E, F) and long burst (Fig. 3A, D) stimulation of ACh release was significantly inhibited by the nonselective muscarinic antagonist atropine. The atropine inhibition coupled with the lack of effect of glutamate and GABA antagonists (Fig. 3A, D) suggest a potential role for M_2 and/or M_3 receptors in mediating the depolarizing responses.

Previous studies have suggested that muscarinic-dependent depolarizing responses in hippocampal pyramidal neurons may result from the inhibition of an M-current (KCNQ channel) (Rouse et al., 2000). To investigate a potential role of the M-current in the depolarizing responses in CA1 interneurons, the KCNQ channel antagonist XE-991 dihydrochloride (2 μM) was bath applied to the slices. SR/SLM interneurons that depolarized enough to fire action potentials in response to ACh release did not cease firing when XE-991 was applied during flashes (n = 6 out of 6, Fig. 3G).

To address whether the synaptically-driven depolarizing response could alter excitatory transmission onto CA1 interneurons, paired pulse electrical stimulation of Schaffer collaterals was delivered before, during, and after depolarizing responses (Fig. 3H). Stimulation before flashes produced a pair of large EPSPs (Fig. 3H, inset left) that failed to produce action potentials in hippocampal interneurons (0 of 5). In contrast, stimulation applied during the synaptically-driven depolarization generated a pair of action potentials (Fig. 3H, inset right) ($n = 5$). Finally, a similar paired pulse following the muscarinic synaptic depolarization failed to produce action potentials (Fig. 3H).

Thus, these data illustrate that synaptically-activated muscarinic receptors on a subset of interneurons can produce depolarizations that increase the excitability of those neurons. Furthermore, these synaptic depolarizations are not due to the activation of M_1, M_4 or M_5 receptors and do not involve the modulation of an M current. Due to a lack of highly selective drugs, however, the role of M_2 and M_3 receptors could not be determined in our assays.

3.4. Synaptically-activated muscarinic biphasic responses

In a subset of interneurons, long duration bursts of light flashes resulted in a fast hyperpolarization (Fig. 4C, arrow indicates max amplitude) followed by a slow depolarization (Fig. 4C, pink box). When flashes ceased, a fast depolarizing point of inflection (Fig. 4C, grey box) occurred in most (78%, 32 of 41) interneurons. This fast depolarizing phase resulted in action potentials in (56%, 23 of 41) of interneurons capable of biphasic responses.

Each interneuron had varying response properties for the hyperpolarizing and depolarizing phases of the biphasic response (Fig. 4A). The majority of interneurons (66%) that had biphasic responses displayed a slow depolarizing phase that was larger in amplitude compared to the hyperpolarizing phase. The remaining interneurons had larger hyperpolarizing phases relative to the depolarizing phase (34%) (Fig. 4B). However, the relative amplitude of the hyperpolarizing to the depolarizing phase varied considerably between interneurons (Fig. 4B). Despite this variability, the mean ratio of depolarization to hyperpolarization across all biphasic responses was 1.02 ± 0.17.

The hyperpolarizing phase of the biphasic response had similar properties to purely hyperpolarizing responses (Figs. 4C and 2). The amplitude of the hyperpolarizing phase was increased 58.8% compared to control levels (Fig. 4F) and the decay of the response (or rise time of the 'after' flash depolarization) was prolonged 58.4% by the M_4 PAM, VU 10010 (Fig. 4D, H). Importantly, the prolongation of the hyperpolarizing phase by VU 10010 was sometimes capable of preventing the emergence of the slow depolarization (2 of 19 cells, Fig. 4E) but more often the M_4 PAM did not have a significant effect on the amplitude of the depolarizing phase (Fig. 4G).

We next investigated a potential role for M_1 or M_5 receptors in the depolarizing or hyperpolarizing phases of the biphasic response. Application of either the M_1 antagonist or M_5 PAM did not have an effect on the amplitude of the hyperpolarizing (Fig. 4F) or depolarizing (Fig. 4G) phases. Additionally, the rise time of the after flash depolarization was not affected by the M_1 antagonist or M_5 PAM (Fig. 4H). Our data suggest that neither M_1 nor M_5 receptors play a role in mediating biphasic responses.

The hyperpolarizing phase of the biphasic responses in CA1 hippocampal pyramidal neurons may be due to the activation of SK channels (Gulledge and Kawaguchi, 2007). To test this in our system, SK channels were blocked by apamin (2 μM). Unlike in pyramidal neurons, apamin did not block the hyperpolarizing phase of the biphasic response nor did it

affect the depolarizing phase (Fig. 4D, F–H). Therefore, our data suggest that the hyperpolarizing phase of the muscarinic biphasic synaptic potentials in interneurons is due to the activation of M_4.

3.5. A subset of biphasic interneurons can be entrained to rhythmically burst

Interneurons that respond to persistent application of muscarinic agonists with oscillating responses have been previously described (McQuiston and Madison, 1999a). However, rhythmic responses due to synaptic release of ACh have not been investigated. Thus we examined the activity of biphasic interneurons when ACh was rhythmically released from presynaptic terminals. We found that a subset of biphasic interneurons (see Fig. 4B, yellow points, 9 of 41 biphasic interneurons) could be entrained to fire bursts of action potentials following rhythmic flashes of blue light (Fig. 5A).

Because the hyperpolarizing phase of the biphasic response was mediated by M_4 receptors, we investigated whether the M_4 PAM could affect the rhythmic entrainment of biphasic interneurons. Bath application of VU 10010 produced a potentiation and prolongation of the hyperpolarizing phase of the biphasic response that resulted in a significant reduction in the number of action potentials produced during each burst (Fig. 5D) and a delay in the time to the first action potential for each burst (Fig. 5B, C). On average, the M_4 PAM significantly delayed the time to the first action potential 977.5 ms ± 165.1 and reduced the number of action potentials per burst by 42.6% ± 12.8. Thus, a subset of biphasic responding interneurons can be entrained to burst by the rhythmic release of ACh. Furthermore, M4 PAMs modulated the properties of these rhythmic bursts.

3.6. Different amounts of presynaptic activity and ACh concentrations are required for different types of postsynaptic responses

As described in the previous experiments, short trains of stimuli (10×20 Hz) were not sufficient to consistently produce the depolarizing component of a biphasic response. This observation suggests that enhanced presynaptic activity and/or larger concentrations of extracellular ACh may be required to produce depolarizing muscarinic synaptic events. Therefore, we investigated the presynaptic activity and extracellular ACh concentration requirements for both depolarizing and hyperpolarizing synaptic responses. By comparing the response amplitudes resulting from short trains of stimuli (Fig. 6A,B left traces, 10×20 Hz) to long trains of stimuli (Fig. 6A,B right traces, 120×20 Hz), we found that hyperpolarizing responses were more likely to be produced by short blue light flashes compared to depolarizing responses (Figs. 6F, 91.1% (51 of 56) hyperpolarization, 41.8% (41 of 99) depolarization). Furthermore, for interneurons that responded to short flashes of blue light, we found that when the number of flashes was increased to 120, the amplitude of the response increased proportionately more for depolarizing responses than for hyperpolarizing responses (Fig. 6C–E, 348% versus 161%, respectively). Therefore, our data suggest that lower levels of presynaptic activity favor the suppression of a subset of interneurons through hyperpolarization whereas higher levels of presynaptic activity recruit a different subset of depolarizing interneurons.

One explanation for the observation that depolarizing muscarinic synaptic responses were more often produced by longer trains of stimuli is that larger concentrations of extracellular ACh are required to activate muscarinic receptors that mediate the depolarizing responses. To test this, we used the acetylcholinesterase inhibitor physostigmine to increase the concentration of extracellular ACh. We found that bath application of physostigmine (10 μM) produced a significant increase in the area measurement of hyperpolarizing and depolarizing responses (Fig. 7C). Although both response types displayed an increase in their average decay time (Fig. 7D), only depolarizing responses displayed an increase in the

average amplitude in the presence of physostigmine (Fig. 7E). Furthermore, the increase in decay time was significantly larger for depolarizing responses than for hyperpolarizing responses, suggesting a differential response to physostigmine that may be explained by the increased extracellular levels of ACh.

3.7. Can the somatic location or Interneuron morphology be correlated with postsynaptic muscarinic response types?

In interneurons that responded to synaptically released ACh ($n = 335$), 79.7% had muscarinic dependent responses while 17.3% had nicotinic-dependent responses (for nicotinic-dependent response see (Bell et al., 2011)). Only 3% of interneurons had responses with both nicotinic and muscarinic components (data not shown). Of the CA1 interneurons that displayed synaptic muscarinic responses, depolarizing responses were the most prevalent (40%) followed by hyperpolarizing (35%) and biphasic (25%) responses (Fig. 8K). However, the proportion of the different response types (hyperpolarizing, depolarizing, and biphasic) varied depending upon the anatomical layer in which the interneuron cell body resided. 74% of interneurons whose cell bodies resided between *stratum pyramidale* (SP) and the alveus (*stratum oriens*, SO) had responses with hyperpolarizing components (hyperpolarization + biphasic responses) whereas the majority (83%) of interneurons in *stratum lacunosum-moleculare* (SLM) and *stratum radiatum* (SR) had a depolarizing component (depolarization + biphasic responses) (Fig. 8K).

It has been suggested that morphologically identified interneuron subclasses serve specific functions depending on brain state (Klausberger and Somogyi, 2008). To identify whether particular response types could be correlated to known morphological classes of interneurons, biocytin was added to our patch pipette and filled cells were reconstructed *post hoc* from confocal images. While we found that the response type was correlated to the soma location (Fig. 8K), we could not correlate specific response types to discrete morphological subclasses of interneurons. Because the extent of biocytin fills varied from cell to cell, precise identification of interneuron subclasses was not possible for all reconstructed cells. For most cells, we designated them as dendritically or somatically projecting interneurons. However, we were able to determine that individual somatically projecting neurons (likely parvalbumin basket cells) had responses that were depolarizing (Fig. 8E), hyperpolarizing (Fig. 8H,I), or biphasic (not shown). Furthermore, individual SLM/SR interneurons with dendritic projections could also be either hyperpolarizing (Fig. 8J), depolarizing (Fig. 8F,G), or biphasic (Fig. 8D). Thus, our results demonstrate that the morphology of an interneuron does not predict an interneuron's response to synaptically released ACh.

3.8. Postsynaptic muscarinic response types do not have specific electrophysiological phenotypes

We characterized the electrophysiological properties of interneurons displaying muscarinic responses by injecting depolarizing and hyperpolarizing currents. We attempted to categorize interneurons based on their firing patterns in response to supra-threshold depolarizing current injections and by the presence or absence of a depolarizing sag in the membrane potential in response to hyperpolarizing current injections.

Each interneuron was classified by three independent measures (Table 1). First (Table 1 left two columns) we classified interneurons on their firing frequency as either fast spiking (FS) or not fast spiking (non-FS). Second (Table 1 middle two columns) we classified interneurons as either producing an accommodating or non-accommodating train of action potentials. And third (Table 1 right two columns) we classified interneurons as producing or not producing a depolarizing sag in the membrane potential in response to a hyperpolarizing

current injection. Fast spiking interneurons, classified by firing rates of greater than 200 Hz in response to a 200 pA depolarizing current, were observed for each of the three synaptic muscarinic response types (Fig. 9A–C). Accommodation of APs was classified by the ratio of the initial and last inter-AP interval. Interneurons with ratios greater than 1.2 were considered accommodating while interneurons with ratios less than 1.2 were considering non-accommodating. Accommodating and non-accommodating interneurons were found for each response type (Table 1). In addition, interneurons could not be classified by the presence or absence of a depolarizing sag in response to hyperpolarizing current injection. Interneurons with (Fig. 9D–F) and without (Fig. 9A–C) a depolarizing sag were found for all response types (Table 1). Furthermore, of the 9 biphasic interneurons capable of being entrained by rhythmic release of ACh, 5 interneurons (Fig. 9F) had a depolarizing sag while 4 interneurons (Fig. 9C) did not.

4. Discussion

Previous studies have shown that muscarinic receptor activation in CA1 interneurons is capable of producing three types of responses: hyperpolarizing, depolarizing, and biphasic responses (McQuiston and Madison, 1999a; Widmer et al., 2006). Our results demonstrate that the probability of producing a particular response depends on the presynaptic activity of cholinergic MS/DBB nerve terminals. In particular, synaptic muscarinic depolarizing responses required more presynaptic activity than that required to produce hyperpolarizing responses. Thus low levels of activity in cholinergic MS/DBB neurons would be expected to mainly suppress a subset of hyperpolarizing interneurons whereas increased amounts of cholinergic MS/DBB activity may recruit a different subset of interneurons with depolarizing responses. Furthermore, a subset of biphasic responding interneurons could be entrained to burst by the rhythmic activation of cholinergic terminals. The requirement for more activity to produce muscarinic depolarizing responses resulted in part from a need for higher ACh extracellular concentrations for their full activation. In addition, the kinetics of the different response types varied. Hyperpolarizing responses were faster (more phasic-like) and depolarizing responses were slower and more prolonged (tonic-like). Pharmacologically, the muscarinic synaptic hyperpolarizing responses were mediated by the activation of M_4 receptors whereas muscarinic receptors mediating the depolarizing synaptic responses could not be identified although M_1, M_4, or M_5 receptors do not appear to be involved. Despite interneurons having different functional and pharmacological synaptic muscarinic responses, interneuron response types did not correlate with known morphological or physiological classifications for CA1 interneurons.

4.1. Different response types require different presynaptic activity

The firing rates of cholinergic neurons in the MS/DBB during different brain states remain unknown. Initial studies that used extracellular action potential waveforms as a method to identify cholinergic neurons in the MS/DBB have suggested that MS/DBB cholinergic neurons fire at approximately 20 Hz and can fire burst of action potentials with instantaneous frequencies greater than 100 Hz during theta rhythms (Brazhnik and Fox, 1997, 1999; King et al., 1998). These data are consistent with the firing behavior of anatomically identified basal forebrain cholinergic neurons that innervate the neocortex (Manns et al., 2000, 2003; Lee et al., 2005). In contrast, more recent studies using *in vivo* juxtacellular recordings have suggested that MS/DBB cholinergic neurons fire at low frequencies (<4 Hz) (Simon et al., 2006). However, these latter studies were limited to four anatomically identified MS/DBB cholinergic neurons. Thus, there may be a subset of MS/DBB cholinergic neurons that fire at higher frequencies and burst during theta rhythms that were not detected by these studies. Our data suggests that a small number of presynaptic action potentials will preferentially hyperpolarize a subset of interneurons. Increasing the number of action potentials will enhance the excitability of a different subset of interneurons

through direct muscarinic depolarization. And finally, depending on the firing pattern of MS/DBB cholinergic neurons, some interneurons may be entrained to burst through the rhythmic release of ACh. However, because it remains unclear how MS/DBB cholinergic neurons fire in awaked behaving animals, it is unknown whether imposed rhythms actually occur *in vivo*. But the biphasic nature of some of these interneurons may permit MS/DBB cholinergic activity to dynamically regulate the activity biphasic interneurons on the timescale of hundreds of milliseconds to seconds.

4.2. Different response types require different concentrations of extracellular ACh and have different kinetics

Our data have demonstrated that a larger number of presynaptic action potentials were required to produce muscarinic depolarizing synaptic potentials compared to hyperpolarizing synaptic responses in hippocampal CA1 interneurons. Furthermore, elevating extracellular concentrations of ACh through the use of an acetylcholinesterase inhibitor increased muscarinic synaptic depolarizations to a significantly greater extent than hyperpolarizations. Taken together, these observations suggest that muscarinic receptors mediating the synaptic depolarization are not saturated whereas those mediating the synaptic hyperpolarization may be closer to saturation following the release of ACh. These observations can be interpreted in a number of ways. First, muscarinic receptor subtypes mediating these two different synaptic responses may have different affinities for ACh. However, it remains unclear whether the five types of muscarinic receptors have different affinities for ACh (Hulme et al., 1990). Second, muscarinic receptors mediating depolarizing responses may be located further away from ACh release sites than those receptors mediating hyperpolarizing synaptic responses. Indeed, only 7% of cholinergic terminals in the hippocampus (Umbriaco et al., 1995) and 15% in the neocortex (Umbriaco et al., 1994) were demonstrated to have postsynaptic specializations: ACh's action on neurons was thought to be via volume transmission (Descarries et al., 1997) rather than classical synaptic activation. However, others have found that the majority of cholinergic terminals (66%) in the neocortex do appear to form classical synapses with post-synaptic specializations (Turrini et al., 2001). Thus, it remains possible that ACh release sites that produce hyperpolarizing responses are classical synapses whereas depolarizing interneurons respond to ACh through volume transmission. One other possible mechanism to explain our findings may be that there is a differential distribution of acetylcholinesterase throughout the hippocampus (Vijayan, 1979). It is possible that ACh release sites and muscarinic receptors mediating hyperpolarizing responses may be surrounded by lower concentrations of acetylcholinesterase. This would effectively increase the concentration of ACh near cholinergic terminals that produce hyperpolarizing responses relative to terminals that produce depolarizing responses.

Our data have also demonstrated that cholinergic synaptic depolarizations and hyperpolarizations differed in their kinetics. More specifically, hyperpolarizations had faster rates of rise and decay times. These observations may result from a variety of mechanisms. First, the differences in the kinetics could be explained by the location of the muscarinic receptors mediating the two different responses. Receptors mediating the muscarinic synaptic depolarizing responses may be located further away from ACh release sites therefore requiring more time for diffusion and therefore a slower rise time. Because depolarizing synaptic responses typically required more presynaptic action potentials, ACh terminals mediating the postsynaptic depolarizing responses may have a lower probability of release thereby producing a slower rise in extracellular ACh concentrations. Finally, the differences in kinetics may be due to the receptor-effector mechanisms mediating the different response types. The interneuron hyperpolarizing synaptic response has been shown to be mediated by the activation of an inwardly rectifying potassium channel (McQuiston

and Madison, 1999a). This likely involves direct G-protein coupling between G_i and a potassium channel (Brown, 2010). In contrast, the mechanism producing the depolarizing synaptic response remains unknown; however, the mechanism mediating the depolarization may involve a cascade of intracellular events that requires more time to produce an electrophysiological response.

4.3. Muscarinic receptor subtypes mediating the different synaptic potentials

All five muscarinic receptor subtypes are expressed in the hippocampus (Wall et al., 1992). Our pharmacological data has shown that M_4 receptors mediate, at least in part, the muscarinic synaptic hyperpolarization in hippocampal CA1 interneurons. Although the muscarinic receptor subtype mediating the synaptic depolarization could not be unequivocally identified pharmacologically, the depolarization is likely mediated by either the M_2 or M_3 receptor. Unfortunately, the proximity of different muscarinic subtypes in the hippocampus relative to their corresponding cholinergic terminals is unknown. However, evidence from striatum suggests that M_4 receptors are found in postsynaptic densities whereas M_1 and M_3 are found mostly extrasynaptically in both striatum (Hersch et al., 1994) and neocortex (Mrzljak et al., 1993). If the hippocampus has a similar distribution of muscarinic receptors as striatum and neocortex, then our pharmacological data strengthens the hypothesis that the hyperpolarizing synaptic responses are faster and require less transmitter release due to the closer proximity of M_4 receptors to presynaptic terminal release sites.

4.4. Muscarinic dependent synaptic responses do not correlate with known morphological or physiological classes of CA1 interneurons

Hippocampal interneurons have been classified into different subtypes based on their morphology, synaptic connectivity, neurotransmitter content, firing properties, and responses to neurotransmitters (Freund and Buzsaki, 1996; Parra et al., 1998; Klausberger and Somogyi, 2008). Previous studies that attempted to correlate interneuron morphology to muscarinic responses failed to show any morphological correlation (Parra et al., 1998; McQuiston and Madison, 1999b, 1999a). However, other studies have suggested that some morphological classes of interneurons do correlate with muscarinic receptor driven changes in interneuron excitability (McMahon et al., 1998; Lawrence et al., 2006; Cea-del Rio et al., 2010, 2011). Using morphological classifications, we did not find correlations between interneuron axonal or dendritic projections and muscarinic response type. Hyperpolarizing, depolarizing and biphasic responses were found in interneurons with perisomatic or dendritic axonal projections. In contrast, we did find a correlation between soma position and response type. More specifically, SO interneurons (which contain both perisomatic and dendritic projecting interneurons) were more likely to have a hyperpolarizing component and SLM/SR interneurons were more likely to have a depolarizing component in their muscarinic synaptic response.

Attempts have been made to classify hippocampal interneurons based on their electrophysiological properties (Freund and Buzaski, 1996). In an attempt to determine whether interneurons with different muscarinic synaptic responses belonged to a specific physiological class of hippocampal interneuron, we examined each interneuron's firing patterns (fast spiking vs regular spiking and accommodating vs non accommodating) and passive electrophysiological responses (presence or absence of a depolarizing sag during hyperpolarizing current injections). Our data showed that the muscarinic synaptic response types could not be specifically correlated with any of the measured electrophysiological properties. Therefore, interneurons with different muscarinic synaptic responses do not belong to discrete electrophysiological classes.

5. Conclusions

We have demonstrated that MS/DBB cholinergic inputs can engage different subsets of hippocampal interneurons depending on MS/DBB cholinergic terminal activity and hippocampal ACh concentrations. Furthermore, treatment with acetylcholinesterase inhibitors does not uniformly increase cholinergic effects, but instead has a larger impact on interneuron subsets depolarized by synaptic muscarinic receptor activation. In contrast, specific subsets of interneurons hyperpolarized by synaptic muscarinic receptor activation could be selectively potentiated by M_4 positive allosteric modulators. These findings may have broader implications as methods are developed to improve cholinergic function in the treatment of neurological diseases involving cholinergic dysfunction such as Alzheimer's disease.

Acknowledgments

Abbreviations

ACh	acetylcholine
ANOVA	analysis of variance
ANT	antagonist
AP	action potential
APV	DL-2-Amino-5-phosphonopentanoic acid
BIC	bicuculline
CA1	cornu ammon 1
Chat	choline acetyltransferase
DIC	differential interference contrast
DNQX	6,7-Dinitroquinoxaline-2,3-dione
EPSP	excitatory postsynaptic potential
IPSP	inhibitory postsynaptic potential
LED	light emitting diode
MS/DBB	medial septum/diagonal band of Broca complex
PAM	positive allosteric modulator
rAAV	recombinant adeno-associated virus
SC	Schaffer collateral
SEM	standard error of the mean
SLM	stratum lacunosum-moleculare
SO	stratum oriens
SP	stratum pyramidale
SR	stratum radiatum

References

Atri A, Sherman S, Norman KA, Kirchhoff BA, Nicolas MM, Greicius MD, Cramer SC, Breiter HC, Hasselmo ME, Stern CE. Blockade of central cholinergic receptors impairs new learning and increases proactive interference in a word paired-associate memory task. Behav Neurosci. 2004; 118:223–236. [PubMed: 14979800]

Bell KA, Shim H, Chen CK, McQuiston AR. Nicotinic excitatory post-synaptic potentials in hippocampal CA1 interneurons are predominantly mediated by nicotinic receptors that contain 4 and 2 subunits. Neuropharmacology. 2011; 61:1379–1388. [PubMed: 21878344]

Blokland A, Honig W, Raaijmakers WG. Effects of intra-hippocampal scopolamine injections in a repeated spatial acquisition task in the rat. Psychopharmacology. 1992; 109:373–376. [PubMed: 1365638]

Bonner TI. New subtypes of muscarinic acetylcholine receptors. Trends Pharmacol Sci. 1989; (Suppl: 11–15)

Brazhnik ES, Fox SE. Intracellular recordings from medial septal neurons during hippocampal theta rhythm. Exp Brain Res. 1997; 114:442–453. Experimentelle Hirnforschung Expérimentation Cérébrale. [PubMed: 9187280]

Brazhnik ES, Fox SE. Action potentials and relations to the theta rhythm of medial septal neurons in vivo. Exp Brain Res. 1999; 127:244–258. Experimentelle Hirnforschung Expérimentation Cérébrale. [PubMed: 10452212]

Bridges TM, Phillip Kennedy J, Noetzel MJ, Breininger ML, Gentry PR, Conn PJ, Lindsley CW. Chemical lead optimization of a pan Gq mAChR M1, M3, M5 positive allosteric modulator (PAM) lead. Part II: development of a potent and highly selective M1 PAM. Bioorg Med Chem Lett. 2010; 20:1972–1975. [PubMed: 20156687]

Bridges TM, Marlo JE, Niswender CM, Jones CK, Jadhav SB, Gentry PR, Plumley HC, Weaver CD, Conn PJ, Lindsley CW. Discovery of the first highly m5-preferring muscarinic acetylcholine receptor ligand, an M5 positive allosteric modulator derived from a series of 5-Trifluoromethoxy N-Benzyl Isatins. J Med Chem. 2009; 52:3445–3448. [PubMed: 19438238]

Brown DA. Muscarinic acetylcholine receptors (mAChRs) in the nervous system: some functions and mechanisms. J Mol Neurosci. 2010; 41:340–346. [PubMed: 20446119]

Caccamo A, Oddo S, Billings LM, Green KN, Martinez-Coria H, Fisher A, LaFerla FM. M1 receptors play a central role in modulating AD-like pathology in transgenic mice. Neuron. 2006; 49:671–682. [PubMed: 16504943]

Cea-del Rio CA, Lawrence JJ, Erdelyi F, Szabo G, McBain CJ. Cholinergic modulation amplifies the intrinsic oscillatory properties of CA1 hippocampal cholecystokinin-positive interneurons. J Physiol (Lond). 2011; 589:609–627. [PubMed: 21115639]

Cea-del Rio CA, Lawrence JJ, Tricoire L, Erdelyi F, Szabo G, McBain CJ. M3 muscarinic acetylcholine receptor expression confers differential cholinergic modulation to Neurochemically distinct hippocampal basket cell subtypes. J Neurosci. 2010; 30:6011–6024. [PubMed: 20427660]

Chiang PH, Yeh WC, Lee CT, Weng JY, Huang YY, Lien CC. M(1)-like muscarinic acetylcholine receptors regulate fast-spiking interneuron excitability in rat dentate gyrus. Neuroscience. 2010; 169:39–51. [PubMed: 20433901]

Dasari S, Gulledge AT. M1 and M4 receptors modulate hippocampal pyramidal neurons. J Neurophysiol. 2011; 105:779–792. [PubMed: 21160001]

Descarries L, Gisiger V, Steriade M. Diffuse transmission by acetylcholine in the CNS. Prog Neurobiol. 1997; 53:603–625. [PubMed: 9421837]

Fornari RV, Moreira KM, Oliveira MG. Effects of the selective M1 muscarinic receptor antagonist dicyclomine on emotional memory. Learn Mem. 2000; 7:287–292. [PubMed: 11040260]

Freund TF, Buzsaki G. Interneurons of the hippocampus. Hippocampus. 1996; 6:347–470. [PubMed: 8915675]

Garber, J. Guide for the Care and Use of Laboratory Animals. National Academy Press; 2011.

Gu Z, Yakel JL. Timing-dependent septal cholinergic induction of dynamic hippocampal synaptic plasticity. Neuron. 2011; 71:155–165. [PubMed: 21745645]

Gulledge AT, Kawaguchi GJ. Phasic cholinergic signaling in the hippocampus: functional homology with the neocortex? Hippocampus. 2007; 17:327–332. [PubMed: 17407133]

Hangya B, Li Y, Muller RU, Czurkó A. Complementary spatial firing in place cell-interneuron pairs. J Physiol (Lond). 2010; 588:4165–4175. [PubMed: 20819942]

Hasselmo ME. The role of acetylcholine in learning and memory. Curr Opin Neurobiol. 2006; 16:710–715. [PubMed: 17011181]

Hersch SM, Gutekunst CA, Rees HD, Heilman CJ, Levey AI. Distribution of m1–m4 muscarinic receptor proteins in the rat striatum: light and electron microscopic immunocytochemistry using subtype-specific antibodies. J Neurosci. 1994; 14:3351–3363. [PubMed: 8182478]

Hulme EC, Birdsall NJ, Buckley NJ. Muscarinic receptor subtypes. Annu Rev Pharmacol Toxicol. 1990; 30:633–673. [PubMed: 2188581]

King C, Recce M, O'Keefe J. The rhythmicity of cells of the medial septum/diagonal band of Broca in the awake freely moving rat: relationships with behaviour and hippocampal theta. Eur J Neurosci. 1998; 10:464–477. [PubMed: 9749709]

Klausberger T, Somogyi P. Neuronal diversity and temporal dynamics: the unity of hippocampal circuit operations. Science. 2008; 321:53–57. [PubMed: 18599766]

Lawrence JJ, Statland JM, Grinspan ZM, McBain CJ. Cell type-specific dependence of muscarinic signalling in mouse hippocampal stratum oriens interneurones. J Physiol (Lond). 2006; 570:595–610. [PubMed: 16322052]

Lee M-G, Hassani OK, Alonso A, Jones BE. Cholinergic basal forebrain neurons burst with theta during waking and paradoxical sleep. J Neurosci. 2005; 25:4365–4369. [PubMed: 15858062]

Levey AI, Edmunds SM, Koliatsos V, Wiley RG, Heilman CJ. Expression of m1-m4 muscarinic acetylcholine receptor proteins in rat hippocampus and regulation by cholinergic innervation. J Neurosci. 1995; 15:4077–4092. [PubMed: 7751967]

Lin JY, Lin MZ, Steinbach P, Tsien RY. Characterization of engineered channelrhodopsin variants with improved properties and kinetics. Biophys J. 2009; 96:1803–1814. [PubMed: 19254539]

Manns ID, Alonso A, Jones BE. Discharge properties of juxtacellularly labeled and immunohistochemically identified cholinergic basal forebrain neurons recorded in association with the electroencephalogram in anesthetized rats. J Neurosci. 2000; 20:1505–1518. [PubMed: 10662840]

Manns ID, Alonso A, Jones BE. Rhythmically discharging basal forebrain units comprise cholinergic, GABAergic, and putative glutamatergic cells. J Neurophysiol. 2003; 89:1057–1066. [PubMed: 12574480]

Maurer AP, Cowen SL, Burke SN, Barnes CA, McNaughton BL. Phase precession in hippocampal interneurons showing strong functional coupling to individual pyramidal cells. J Neurosci. 2006; 26:13485–13492. [PubMed: 17192431]

McMahon LL, Williams JH, Kauer JA. Functionally distinct groups of interneurons identified during rhythmic carbachol oscillations in hippocampus in vitro. J Neurosci. 1998; 18:5640–5651. [PubMed: 9671655]

McQuiston AR, Madison DV. Muscarinic receptor activity has multiple effects on the resting membrane potentials of CA1 hippocampal interneurons. J Neurosci. 1999a; 19:5693–5702. [PubMed: 10407010]

McQuiston AR, Madison DV. Muscarinic receptor activity induces an afterdepolarization in a subpopulation of hippocampal CA1 interneurons. J Neurosci. 1999b; 19:5703–5710. [PubMed: 10407011]

Moscovitch M, Nadel L, Winocur G, Gilboa A, Rosenbaum RS. The cognitive neuroscience of remote episodic, semantic and spatial memory. Curr Opin Neurobiol. 2006; 16:179–190. [PubMed: 16564688]

Mrzljak L, Levey AI, Goldman-Rakic PS. Association of m1 and m2 muscarinic receptor proteins with asymmetric synapses in the primate cerebral cortex: morphological evidence for cholinergic modulation of excitatory neurotransmission. Proc Natl Acad Sci USA. 1993; 90:5194–5198. [PubMed: 8389473]

Nagode DA, Tang AH, Karson MA, Klugmann M, Alger BE. Optogenetic release of ACh induces rhythmic bursts of perisomatic IPSCs in hippocampus. PLoS ONE. 2011; 6:e27691. [PubMed: 22110723]

Parikh V, Kozak R, Martinez V, Sarter M. Prefrontal acetylcholine release controls cue detection on multiple timescales. Neuron. 2007; 56:141–154. [PubMed: 17920021]

Parra P, Gulyás AI, Miles R. How many subtypes of inhibitory cells in the hippocampus? Neuron. 1998; 20:983–993. [PubMed: 9620702]

Rouse ST, Hamilton SE, Potter LT, Nathanson NM, Conn PJ. Muscarinic-induced modulation of potassium conductances is unchanged in mouse hippocampal pyramidal cells that lack functional M1 receptors. Neurosci Lett. 2000; 278:61–64. [PubMed: 10643801]

Royer, S.; Zemelman, BV.; Losonczy, A.; Kim, J.; Chance, F.; Magee, JC.; Buzsáki, G. Control of Timing, Rate and Bursts of Hippocampal Place Cells by Dendritic and Somatic Inhibition. Nature Publishing Group; 2012.

Schnütgen F, Doerflinger N, Calléja C, Wendling O, Chambon P, Ghyselinck NB. A directional strategy for monitoring Cre-mediated recombination at the cellular level in the mouse. Nat Biotechnol. 2003; 21:562–565. [PubMed: 12665802]

Sheffler DJ, Williams R, Bridges TM, Xiang Z, Kane AS, Byun NE, Jadhav S, Mock MM, Zheng F, Lewis LM, Jones CK, Niswender CM, Weaver CD, Lindsley CW, Conn PJ. A novel selective muscarinic acetylcholine receptor subtype 1 antagonist reduces seizures without impairing hippocampus-dependent learning. Mol Pharmacol. 2009; 76:356–368. [PubMed: 19407080]

Shirey JK, Xiang Z, Orton D, Brady AE, Johnson KA, Williams R, Ayala JE, Rodriguez AL, Wess J, Weaver D, Niswender CM, Conn PJ. An allosteric potentiator of M4 mAChR modulates hippocampal synaptic transmission. Nat Chem Biol. 2008; 4:42–50. [PubMed: 18059262]

Simon AP, Poindessous-Jazat F, Dutar P, Epelbaum J, Bassant M-H. Firing properties of anatomically identified neurons in the medial septum of anesthetized and unanesthetized restrained rats. J Neurosci. 2006; 26:9038–9046. [PubMed: 16943562]

Soares JCK, Fornari RV, Oliveira MGM. Role of muscarinic M1 receptors in inhibitory avoidance and contextual fear conditioning. Neurobiol Learn Mem. 2006; 86:188–196. [PubMed: 16647280]

Turrini P, Casu MA, Wong TP, De Koninck Y, Ribeiro-da-Silva A, Cuello AC. Cholinergic nerve terminals establish classical synapses in the rat cerebral cortex: synaptic pattern and age-related atrophy. NSC. 2001; 105:277–285.

Umbriaco D, Garcia S, Beaulieu C, Descarries L. Relational features of acetylcholine, noradrenaline, serotonin and GABA axon terminals in the stratum radiatum of adult rat hippocampus (CA1). Hippocampus. 1995; 5:605–620. [PubMed: 8646286]

Umbriaco D, Watkins KC, Descarries L, Cozzari C, Hartman BK. Ultra-structural and morphometric features of the acetylcholine innervation in adult rat parietal cortex: an electron microscopic study in serial sections. J Comp Neurol. 1994; 348:351–373. [PubMed: 7844253]

Vijayan VK. Distribution of cholinergic neurotransmitter enzymes in the hippocampus and the dentate gyrus of the adult and the developing mouse. NSC. 1979; 4:121–137.

Volpicelli LA, Levey AI. Muscarinic acetylcholine receptor subtypes in cerebral cortex and hippocampus. Prog Brain Res. 2004; 145:59–66. [PubMed: 14650906]

Wall SJ, Yasuda RP, Li M, Ciesla W, Wolfe BB. Differential regulation of subtypes m1-m5 of muscarinic receptors in forebrain by chronic atropine administration. J Pharmacol Exp Ther. 1992; 262:584–588. [PubMed: 1323653]

Widmer H, Ferrigan L, Davies CH, Cobb SR. Evoked slow muscarinic acetylcholinergic synaptic potentials in rat hippocampal interneurons. Hippocampus. 2006; 16:617–628. [PubMed: 16770798]

Zhang H, Lin S-C, Nicolelis MAL. Spatiotemporal coupling between hippocampal acetylcholine release and theta oscillations in vivo. J Neurosci. 2010; 30:13431–13440. [PubMed: 20926669]

Zheng F, Seeger T, Nixdorf-Bergweiler BE, Alzheimer C. Layer-specific processing of excitatory signals in CA1 interneurons depends on postsynaptic M_2 muscarinic receptors. Neurosci Lett. 2011; 494:217–221. [PubMed: 21396982]
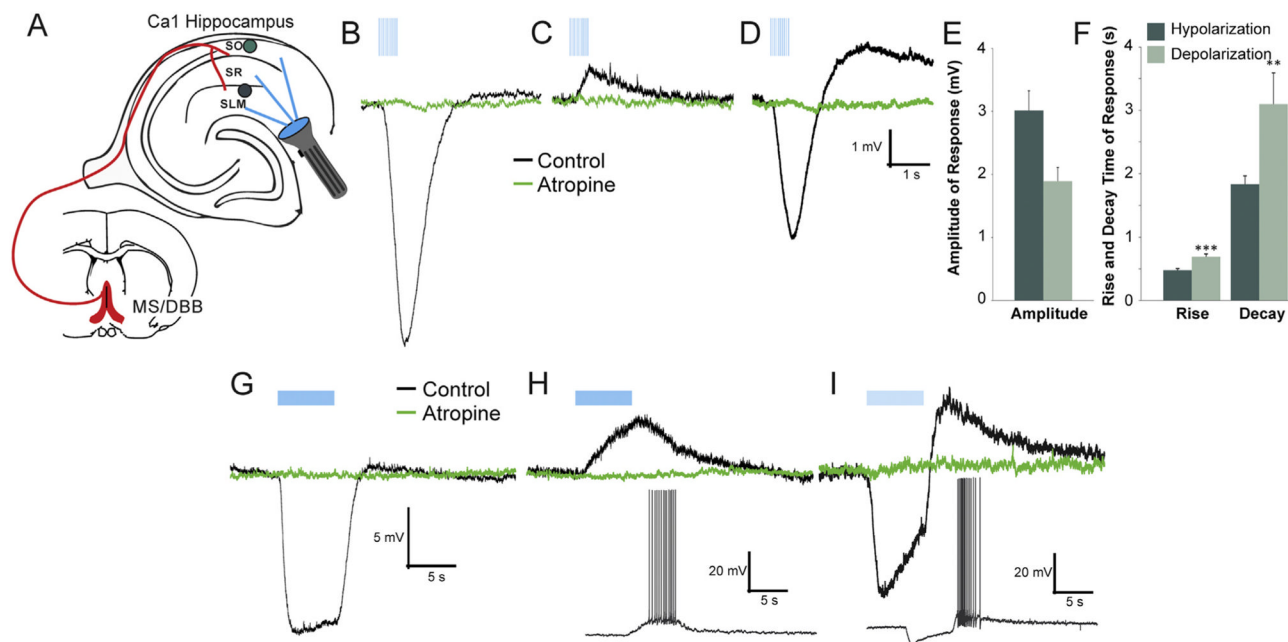
Fig. 1.
Acetylcholine (ACh) release from medial septum/diagonal band of Broca (MS/DBB)
terminals produced three different response types in hippocampal CA1 interneurons. A.
Schematic illustrating experimental system. MS/DBB Chat-Cre neurons were infected with
rAAV-Flex-rev-oChIEF-tdTomato resulting in oChIEF-tdTomato expressing cholinergic
axonal terminals in CA1. ACh release was evoked by blue light flashes. Responses to ACh
release were recorded in CA1 interneurons using whole cell patch clamp techniques. B–D.
ACh release produced muscarinic-dependent responses (black traces) in CA1 interneurons.
Ten light flashes (blue vertical lines, 1 ms duration) at 20 Hz (10×20 Hz) generated either
hyperpolarizing (B), depolarizing (C), or biphasic responses (D) that were blocked by 5 μM
atropine (green traces). E. Histogram showing the average amplitude of the depolarizing (n
$= 49$) and hyperpolarizing ($n = 51$) responses. F. Histogram showing that the average rise
and decay time of depolarizing responses were significantly slower than hyperpolarizing
responses (t-test, rise $p < 0.001$, decay $p < 0.01$). Hyperpolarizing (G), depolarizing (H) and
biphasic responses (I) were also observed when the duration of the flash burst was increased
(120×20 Hz). In some cells, depolarizing (H *inset*) and biphasic (I *inset*) responses to $120 \times$
20 Hz flashes resulted in action potential firing. (For interpretation of the references to color
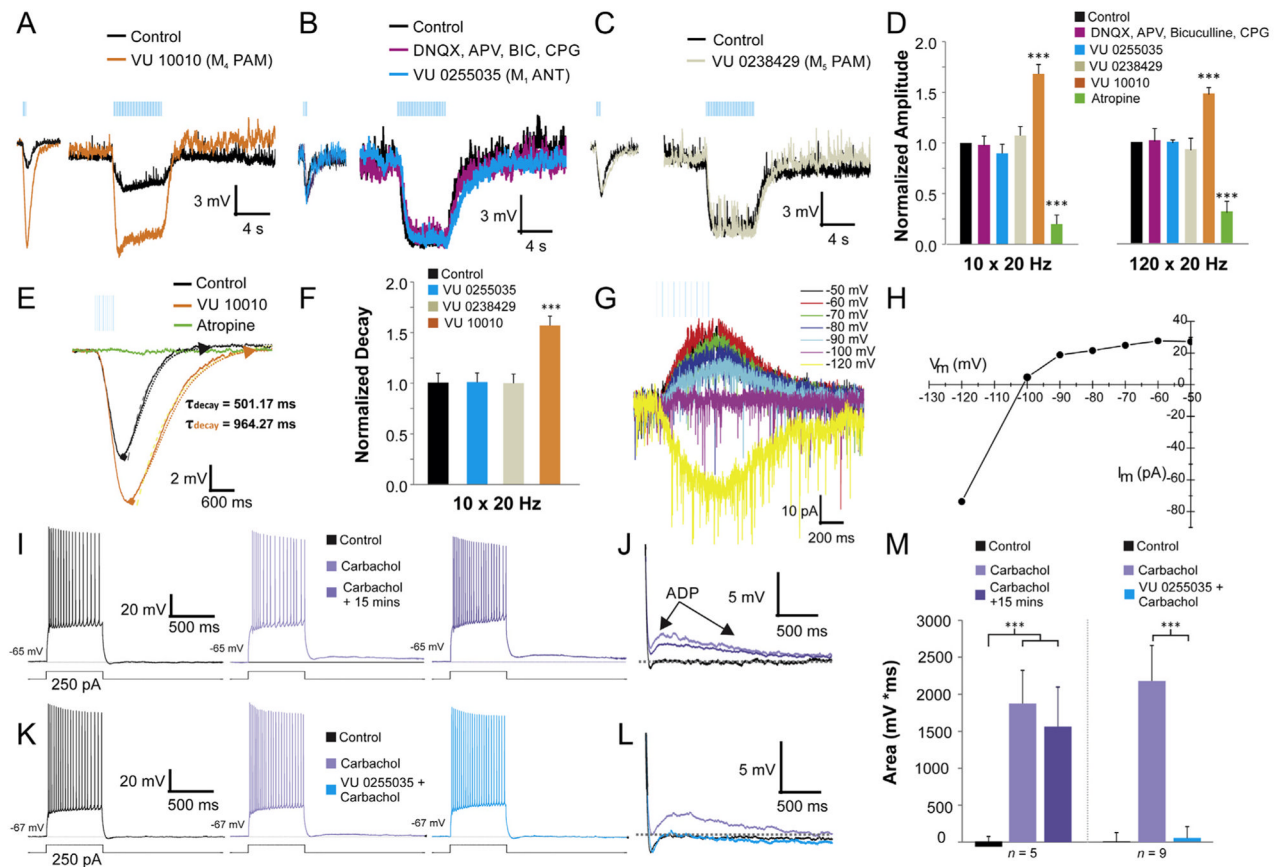in this figure legend, the reader is referred to the web version of this article.)

Fig. 2.

M_4 receptors modulate hyperpolarizing responses in CA1 interneurons. A–C. Muscarinic inhibitory postsynaptic potentials (IPSP) induced by 10 (left traces) and 120 (right traces) blue light flashes at 20 Hz. The M_4 PAM (VU 10010, 5 μM) (A, orange trace) potentiated the IPSP amplitude for both the short trains (10×20 Hz) and prolonged (120×20 Hz) bursts of light. Ionotropic glutamate and $GABA_{A-B}$ receptor antagonists (APV 50 μM, DNQX 30 μM, bicuculline 25 μM, CGP 55845 10 μM) (B, purple trace) did not block the IPSP. M_1 antagonist (VU 0255035, 10 μM) (B, blue trace) and M_5 positive allosteric modulator (PAM) (VU 0238429, 5 μM) (C, grey trace) also had no effect on the IPSP. D. Histogram illustrating the normalized amplitude of muscarinic IPSPs in the presence ionotropic glutamate and $GABA_{A-B}$ receptor antagonists (pink) ($n = 17$), M_1 antagonist (blue) ($n = 11$), M_5 PAM (grey) ($n = 5$), M_4 PAM (orange) ($n = 28$) or atropine (green) ($n = 18$) (one-way ANOVA, $p < 0.001$, Bonferroni post hoc test $p < 0.001$ for atropine and M_4 PAM). E. Example trace illustrating that M_4 PAM prolonged IPSP decay time constant (orange trace). F. Histogram showing that M_4 PAM significantly prolonged the decay time constant of the hyperpolarizing response (one-way ANOVA, $p < 0.001$, Bonferroni post hoc test $p < 0.001$, $n = 20$). G–H. Voltage clamp recordings of the inhibitory muscarinic response held at different potentials. Reversal potential was -105.9 mV, consistent with an inwardly rectifying K^+ current. I. Responses of a CA1 pyramidal neuron to depolarizing current injection (600 ms) before 10 μM carbachol (black traces), 3 min (light purple) and 15 min (dark purple) after 10 μM carbachol. J. Traces in I. expanded and superimposed show the emergence of an afterdepolarization (ADPs) 3 and 15 min post application of carbachol. K. Traces (L, expanded trace showing ADP) demonstrating that the carbachol-induced ADP (purple) was blocked within 3 min of bath application of VU 0255035 (5 μM,

blue). M. Histogram showing carbachol induced an ADP after 3 min of carbachol (middle bars) bath application (one-way ANOVA, $p < 0.001$, Bonferroni post hoc test $p < 0.001$). No difference in the size of the ADP was found between bath application of carbachol 3 and 15 min after application (one-way ANOVA, $p < 0.001$, Bonferroni post hoc test n/s, $n = 5$). In contrast, VU 0255035 significantly blocked the ADP in all pyramidal neurons tested within 3 min of bath application with carbachol (one-way ANOVA, $p < 0.001$, Bonferroni post hoc test $p < 0.001$, $n = 9$). (For interpretation of the references to color in this figure legend, the reader is referred to the web version of this article.)
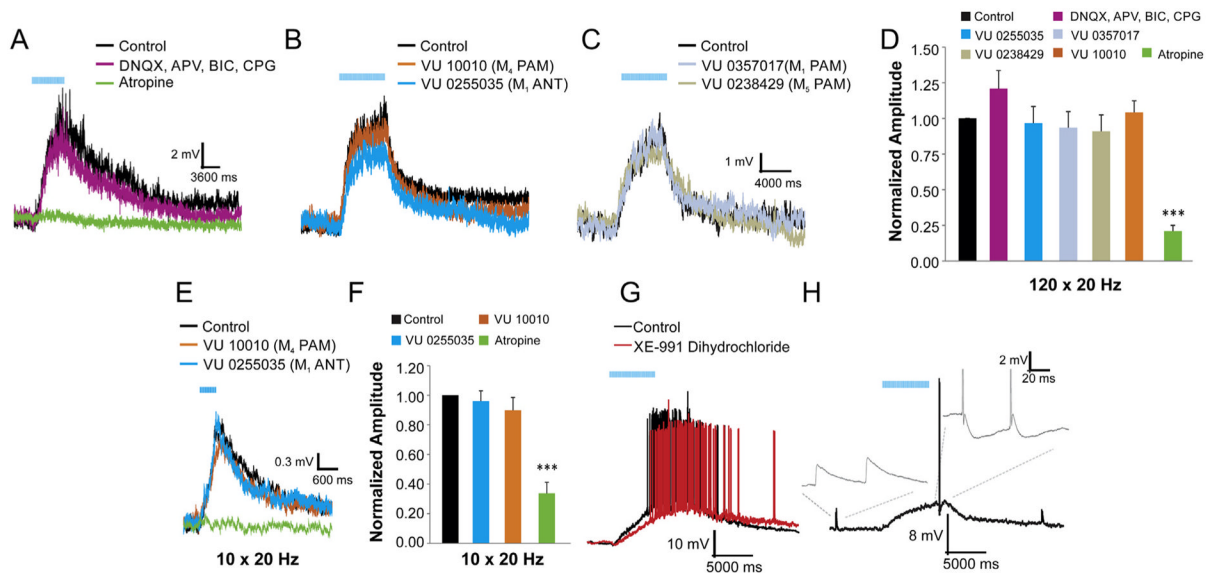
Fig. 3.

Muscarinic-dependent slow depolarization in CA1 interneurons is not mediated by M_1, M_4 or M_5 receptors. A–C. Example of muscarinic excitatory postsynaptic potentials (EPSPs). A. Atropine (green trace) but not ionotropic glutamate and $GABA_{A-B}$ receptor antagonists (purple trace) (APV 50 μM, DNQX 30 μM, bicuculline 25 μM, CGP 55845 10 μM) blocked the EPSPs. B. M_1 antagonist (VU 0255035, 10 μM) (blue trace) ($n = 21$) and M_4 PAM (VU 10010, 5 μM) (orange trace) ($n = 13$) had no effect on the EPSP amplitude. C. M_1 PAM (VU 0357017, 5 μM) (light blue trace) ($n = 11$) and M_5 PAM (VU 0238429, 5 μM) (grey trace) ($n = 7$) also had no effect on the EPSP amplitude. D. Histogram of normalized EPSP amplitudes. Only atropine (5 μM) affected muscarinic EPSPs elicited by 120×20 Hz blue light flashes (one-way ANOVA, $p < 0.01$, Bonferroni post hoc test $p < 0.001$, $n = 15$). E. Example traces of a muscarinic EPSP evoked by 10 flashes at 20 Hz. M_1 antagonist (VU 0255035, 10 μM) ($n = 9$) (E, blue trace) and M_4 PAM (VU 10010, 5 μM) (E, orange trace) ($n = 5$) had no effect on the normalized amplitude of the EPSP (F) Only atropine significantly affected depolarizations evoked by 10 flashes of light (one-way ANOVA, $p < 0.001$, Bonferroni post hoc test $p < 0.001$, $n = 18$). G. Example trace demonstrating that a selective KCNQ channel blocker (XE-991 dihydrochloride, 2 μM) (red trace) did not block the muscarinic-dependent slow depolarization ($n = 6$). H. Muscarinic EPSP converted subthreshold Schaffer-collateral EPSPs into EPSPs that produced action potentials (inset, right) ($n = 5$). Action potentials have been clipped for illustrative purposes. (For interpretation of the references to color in this figure legend, the reader is referred to the web version of this article.)
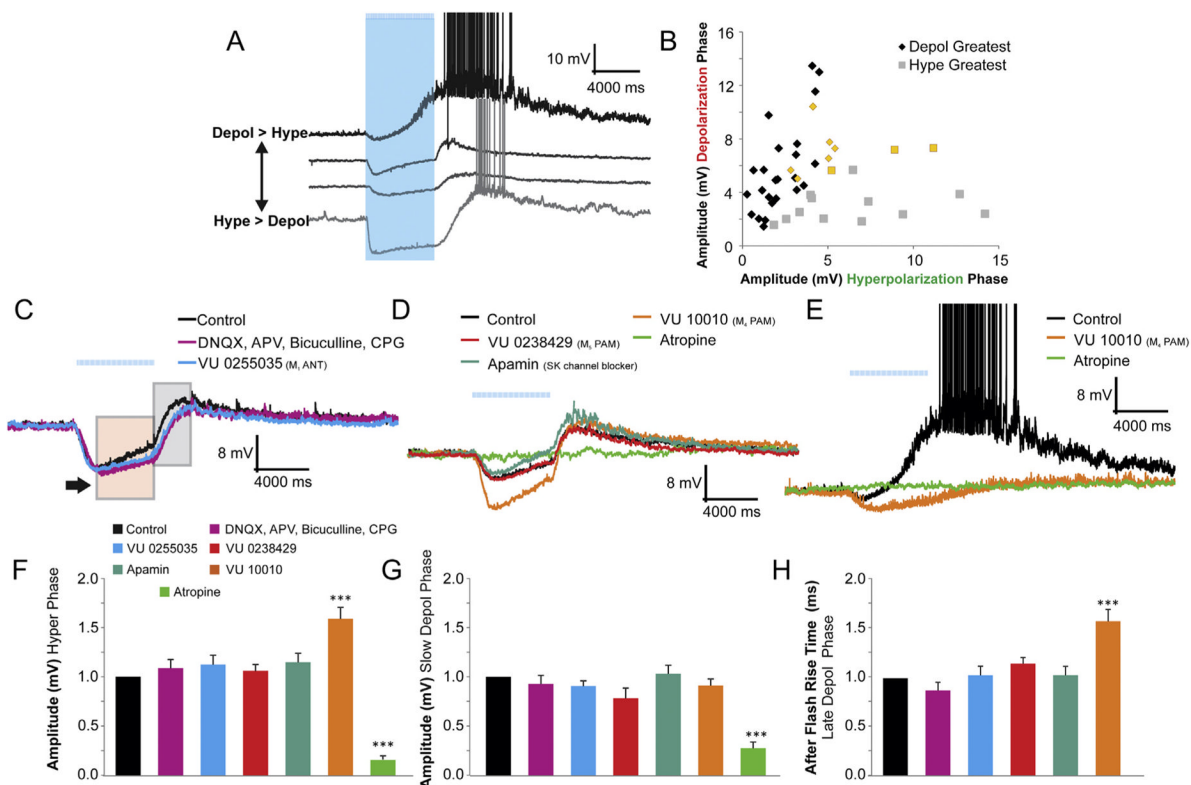
Fig. 4.
Biphasic responses: Variable responses and dependence on M_4-mediated fast hyperpolarizations. A. Four examples of different interneurons with biphasic responses of varying amplitudes and kinetics. B. Plot of the depolarizing amplitude vs. the hyperpolarizing amplitude of interneurons with biphasic responses demonstrates the large variability between cells (yellow – interneurons that had rhythmic biphasic responses – see Fig. 5). C. Traces of biphasic responses with an initial IPSP (amplitude black arrow) followed by a slow depolarizing decay (pink box) in response to 120 blue light flashes at 20 Hz. A post-flash rebound depolarization (grey box) followed the initial slow depolarization. Ionotropic glutamate and $GABA_{A-B}$ receptor antagonists (APV 50 μM, DNQX 30 μM, bicuculline 25 μM, CGP 55845 10 μM) (purple trace) ($n = 10$) did not inhibit either the IPSP or EPSP. M_1 antagonist (VU 0255035, 10 μM) (blue trace) ($n = 6$) also did not block either the IPSP or EPSP. **D**. M_5 PAM (VU 0238429, 5 μM) (red trace) ($n = 6$), and SK channel blocker (apamin, 2 μM) (blue trace) ($n = 6$) had little effect on either the depolarizing or hyperpolarization responses. M_4 PAM (VU 10010, 5 μM) (orange trace) did potentiate the hyperpolarizing amplitude and the rise time of the post flash depolarization ($n = 19$). In some cases (2 of 19), the M_4 PAM effect resulted in the elimination of the slow depolarization (E, action potentials have been clipped). F, G. Histogram of the normalized amplitudes of the depolarizing and hyperpolarizing phases of biphasically responding interneurons. Atropine blocked both the hyperpolarization and the depolarization (one-way ANOVA, $p < 0.01$, Bonferroni post hoc test $p < 0.001$, $n = 12$) whereas the M_4 PAM potentiated the hyperpolarizing amplitude (Bonferroni post hoc test $p < 0.001$, $n = 19$). H. The rise time of the after flash depolarization was significantly increased in the presence of M_4 PAM (one-way ANOVA, $p < 0.001$, Bonferroni post hoc test $p < 0.001$, $n = 19$). (For interpretation of the references to color in this figure legend, the reader is referred to the web version of this article.)
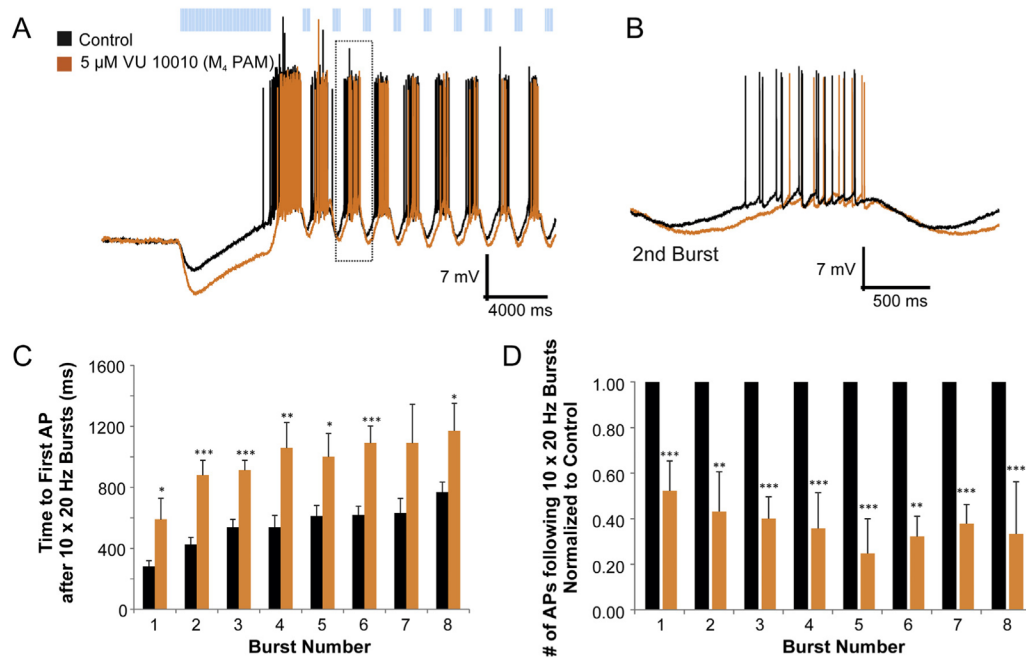
Fig. 5.
A subset of biphasic cells was capable of rhythmic bursting following repetitive ACh synaptic release. A. Current clamp traces of responses to prolonged light flashes (120×20 Hz) followed by short repetitive (0.6 Hz) burst flashes (10×20 Hz) produced phasic bursting of action potentials. Bath application of M_4 PAM increased both the amplitude and decay time of the hyperpolarization phase (A–B, orange trace) ($n = 8$). C. Histogram of the delay to first action potential following a 10×20 Hz burst of blue light. M_4 PAM delayed the firing of the first action potential across most bursts (*t*-test, $p < 0.05$–0.001, $n = 8$). D. Histogram of the number of action potentials per burst. M_4 PAM reduced the total number of action potentials for all eight bursts of light (*t*-test, $p < 0.01$–0.001, $n = 8$).
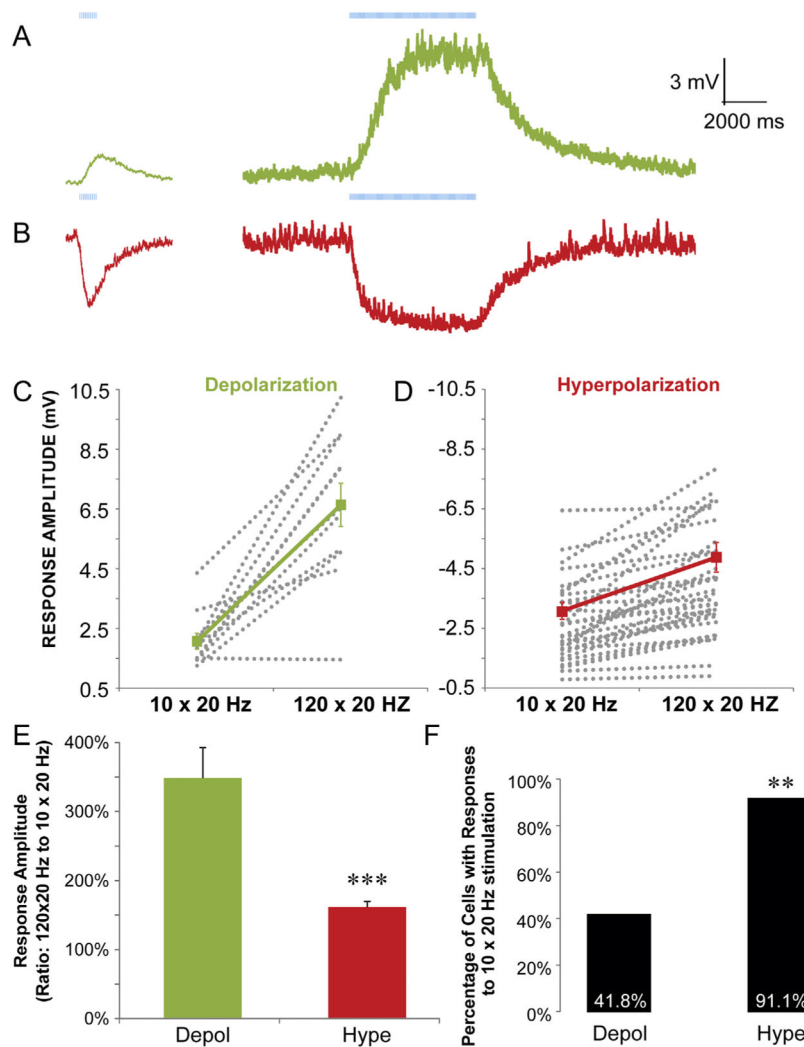
Fig. 6.
Muscarinic EPSPs in CA1 interneurons require more presynaptic activity than muscarinic IPSPs. A–B. Current clamp recordings from interneurons that produced muscarinic depolarizations (A, green traces) or hyperpolarizations (B, red traces) in response to 10 (left traces) and 120 flashes (right traces) at 20 Hz. C-D. Plot of all amplitudes for all interneurons with depolarizing (C) and hyperpolarizing (D) responses to 10 (left) and 120 (right) flashes at 20 Hz (grey, dotted lines). Average amplitudes across all cells are shown by the solid color lines. E. Histogram showing the percent increases in response amplitude when longer trains of flashes were used (120×20 Hz compared to 10×20 Hz flashes). Depolarizing responses showed larger relative increases in response amplitudes with longer trains of flashes (*t*-test, $p < 0.001$, $n = 11$ depol, 23 hype). F. A plot of the percentage of cells with detectable responses to 10×20 Hz flashes for both hyperpolarizing and depolarizing muscarinic responses. There was a higher probability of observing hyperpolarizing muscarinic responses compared to depolarizing responses (*t*-test, $p < 0.01$, $n = 99$ depol, 56 hype). (For interpretation of the references to color in this figure legend, the reader is referred to the web version of this article.)
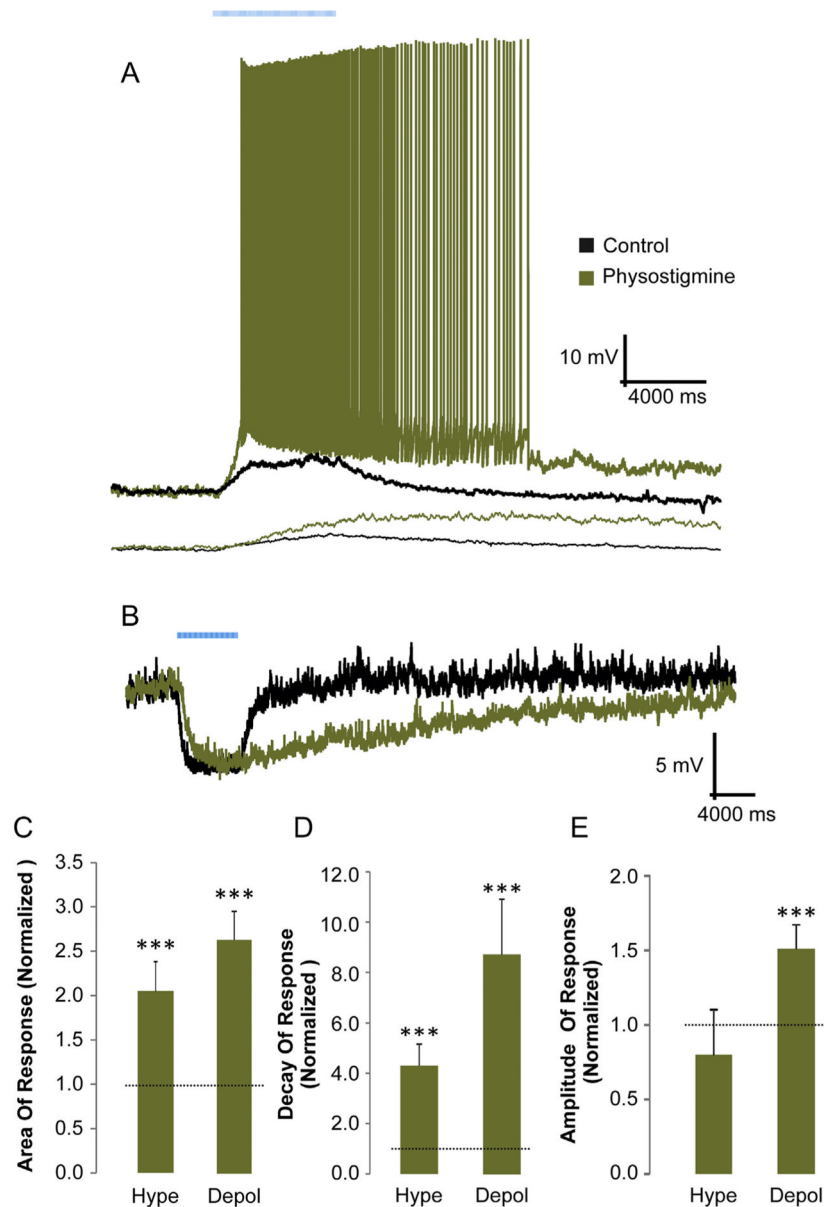
Fig. 7.
Inhibition of acetylcholinesterase increased the amplitude of muscarinic depolarizing but not hyperpolarizing responses. A, B. Current clamp recordings illustrating the effect of acetylcholinesterase inhibitor physostigmine (10 μM) on 2 different depolarizing responses (A) and one hyperpolarizing (B) response. In some cases physostigmine converted a subthreshold depolarizing response into one that evoked action potentials (A top example, 5 of 8 cells). C. Histogram of the area (normalized) of depolarizing and hyperpolarizing muscarinic responses (*t*-test, $p < 0.001$, $n = 10$ depol, 9 hype) D. Histogram of the decay times (normalized) for depolarizing and hyperpolarizing responses. Both depolarizing ($n = 10$) and hyperpolarizing ($n = 9$) areas and decay times were increased significantly increased (*t*-test, $p < 0.001$) by physostigmine. E. Histogram of the normalized amplitude of depolarizing and hyperpolarizing muscarinic responses. Physostigmine significantly

increased depolarizing responses (t-test, $p < 0.001$, $n = 10$) but not hyperpolarizing responses ($n = 9$). Dotted lines (C–E) indicate the normalized unity value.
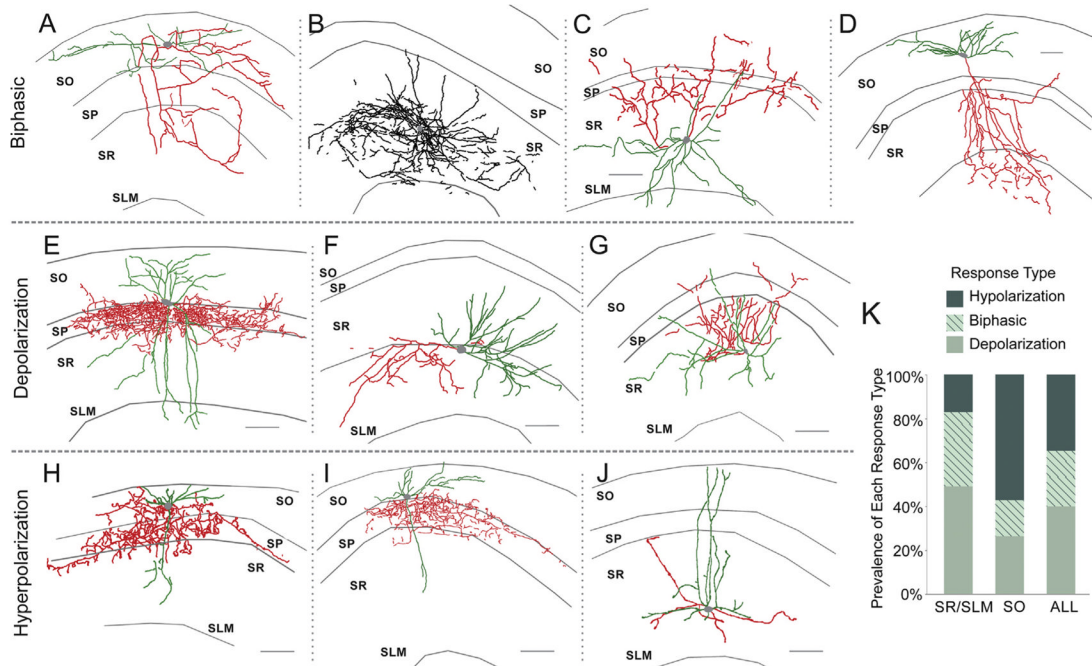
Fig. 8.
Morphology of interneurons with muscarinic synaptic responses. Axonal arborizations are depicted in red and dendrites are depicted in green. In cases where the axonal projection could not be identified from the dendritic projection all projections were labeled in black. Examples of perisomatic projecting SO interneurons that responded to ACh synaptic release with depolarizing (E) and hyperpolarizing (H, I) responses. Examples of dendritically projecting SR/SLM interneurons that responded to ACh synaptic release with biphasic (B), depolarizing (F, G), and hyperpolarizing (J) responses. Example morphology of multilaminar projecting interneurons that responded to ACh synaptic release with biphasic (C) and depolarizing responses (D). (A) Example morphology of a bistratified interneuron that responded to ACh synaptic release with a biphasic response (scale bar = 100 μm). K. Histogram showing a greater number of responses containing a depolarizing component was observed in SR/SLM interneurons (127 of 153 SR/SLM interneurons compared to 42 of 101 SO interneurons, Fisher's Exact Test, two-tailed $p < 0.001$) and more responses with a hyperpolarizing component were found in SO interneurons (76 of 101 SO interneurons compared to 78 of 153 SR/SLM, Fisher's Exact Test, two-tailed $p < 0.001$).
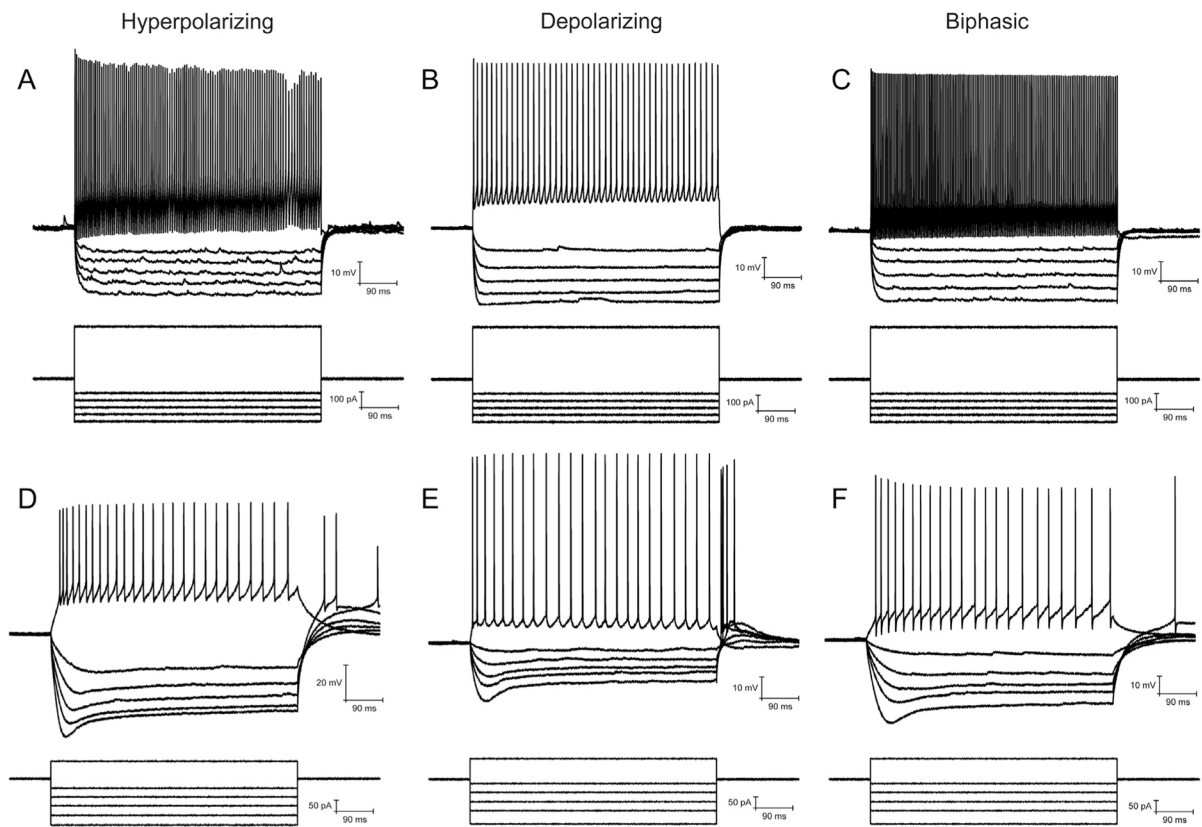
Hyperpolarizing   Depolarizing   Biphasic

Fig. 9.
Active and passive electrophysiological properties of interneurons with muscarinic synaptic responses. Example of fast spiking interneurons that displayed hyperpolarizing (A), depolarizing (B), and biphasic (C) muscarinic synaptic responses. Example of interneurons with depolarizing sag that displayed hyperpolarizing (D), depolarizing (E), and biphasic (F) muscarinic synaptic responses.

Table 1

Electrophysiological properties of interneurons with different muscarinic response types.

	FS	Non-FS	Accommodating	Non-accommodating	Sag	No sag
Hyperpolarizing	22 (51.2%)	21 (48.8%)	27 (62.8%)	16 (37.2%)	24 (55.8%)	19 (44.2%)
Depolarizing	15 (26.8%)	41 (73.2%)	40 (71.4%)	16 (28.6%)	35 (61.4%)	22 (38.6%)
Biphasic	10 (31.3%)	22 (68.8%)	23 (71.9%)	9 (28.1%)	12 (37.5%)	20 (62.5%)